

Effective field theory of Bose–Einstein condensation of α clusters and Nambu–Goldstone–Higgs states in ^{12}C

Y. Nakamura,^{1,2,*} J. Takahashi,^{1,†} Y. Yamanaka,^{1,‡} and S. Ohkubo^{3,4,§}

¹*Department of Electronic and Physical Systems, Waseda University, Tokyo 169-8555, Japan*

²*Nagano Prefectural Kiso Seiho High School, Nagano 397-8571, Japan*

³*Research Center for Nuclear Physics, Osaka University, Ibaraki, Osaka 567-0047, Japan*

⁴*University of Kochi, Kochi 780-8515, Japan*

(Dated: June 8, 2021)

An effective field theory of α cluster condensation is formulated as a spontaneously broken symmetry in quantum field theory to understand the *raison d'être* and nature of the Hoyle and α cluster states in ^{12}C . The Nambu–Goldstone and Higgs mode operators in infinite systems are replaced with a pair of canonical operators whose Hamiltonian gives rise to discrete energy states in addition to the Bogoliubov–de Gennes excited states. The calculations reproduce well the experimental spectrum of the α cluster states. The existence of the Nambu–Goldstone–Higgs states is demonstrated and crucial. The γ decay transitions are also obtained.

PACS numbers: 21.60.Gx, 27.20.+n, 67.85.De, 03.75.Kk

I. INTRODUCTION

Alpha cluster condensation in nuclei has attracted much attention since the observation of Bose–Einstein condensation (BEC) of trapped cold atoms [1]. In ^{12}C , the three- α structure was most thoroughly investigated by Uegaki *et al.* [2], who showed that the 0_2^+ state at an excitation energy E_x of 7.654 MeV, the Hoyle state, which is crucial for nucleosynthesis, the evolution of stars, and the emergence of life, has a dilute structure in a new “ α -boson gas phase” and clarified the systematic existence of a “new phase” of three α clusters above the α threshold. The Hoyle state has been extensively studied theoretically [3–13] and experimentally [14–21], and has been considered widely as an α cluster condensate. It has a gas-like structure with a dilute matter distribution of three- α clusters, 70% of which are in the $0s$ state [6]. However, no firm evidence of BEC, such as superfluidity, has been found.

In ^{12}C , all the excited states except the 2_1^+ state at 4.44 MeV appear above the α particle threshold (7.367 MeV). Recently, α cluster states above the Hoyle state, which are also candidates for an α cluster condensate, that is, the 0_3^+ state at 9.04 MeV, 0_4^+ state at 10.56 MeV, 2_2^+ state (~ 9.75 MeV) [14–18], and 4_1^+ state (~ 13.3 MeV) [19, 20] have been observed. To date, studies using α cluster models [6–8] and *ab initio* calculations [9–13] explain the Hoyle state and the excited gas-like states as collective states of α clusters or nucleons in *configuration space*. Collective motions arise owing mostly to spontaneously broken symmetries (SBSs) in the configuration space, such as rotational and translational ones, or in

the gauge space [22, 23]. The BEC of α clusters is a manifestation of the SBS of the global phase. It would be difficult from the standpoint of traditional α cluster models or *ab initio* calculations to conclude that BEC is truly realized, because it is not clear then what type of *symmetry* is broken for the Hoyle state and the α condensate states above it.

In the study of α cluster condensation, it is important to treat the SBS of the global phase on the basis of quantum field theory because of its unifying view and underlying principle. SBS is ubiquitous [24]; when it occurs, a Nambu–Goldstone (NG) mode (phason) appears according to the NG theorem [25, 26], and a Higgs (amplitude) mode (amplitudon) usually accompanies it. For example, in infinite superconducting systems, the NG mode [27], which is eaten by the plasmon, and the Higgs mode [28, 29] have been observed. For systems with a finite particle number, both the NG and Higgs modes have been confirmed in superfluid nuclei as a pairing rotation and pairing vibration, respectively [30]. The observation of the Higgs boson in particle physics [31] has stimulated a search for Higgs modes in other phenomena, including a recent experiment on Higgs mode excitation in a superconductor using a terahertz pulse [32]. It is intriguing to reveal the emergence of the NG and Higgs modes theoretically in an α cluster condensate and to observe them experimentally. Because the system is finite in size and particle number, they would manifest themselves not as particle excitations but as resonant states with discrete energy levels. From this viewpoint, Ref.[33] discussed a possible emergence of such states for an α cluster condensate in ^{12}C and ^{16}O qualitatively.

The purpose of this paper is to show for the first time that the dilute excited α cluster states, the Hoyle state and those above it, can be understood as new discrete states that follow naturally in the formulation of quantum field theory [34], called the interacting zero mode formulation (IZMF in short), for BEC of α clusters in terms of the field equation, canonical commutation rela-

* yusuke.n@asagi.waseda.jp

† j.takahashi@aoni.waseda.jp

‡ yamanaka@waseda.jp

§ shigeo.ohkubo@rcnp.osaka-u.ac.jp

tions (CCRs), and global gauge invariance.

This paper is organized as follows. In Sect. II, the IZMF for BEC of trapped cold atoms is extended to BEC of α clusters. In Sect. III, we introduce a phenomenological model of α clusters, in which α particles are trapped by a harmonic potential and the α - α interaction is described by a phenomenological Ali-Bodmer potential [35]. Then, the strengths of the harmonic potential and the repulsive potential in the Ali-Bodmer potential are the key parameters in our analysis. We calculate the energy levels, adjusting the two parameters, and compare them with the observed α cluster states. The γ decay transition probabilities are calculated in Sect. V. Sect. VI is devoted to the summary.

II. FORMULATION OF QUANTUM FIELD THEORY OF BOSE-EINSTEIN CONDENSATION FOR α CLUSTERS

First, we clarify from quantum field theory for the α cluster condensate that the canonical operators [34], which replace the NG and Higgs mode operators in infinite systems with SBS, emerge and that the spectrum of their quantum mechanical system is discrete.

We start with the following Hamiltonian for the α cluster system described by the field operator $\hat{\psi}$:

$$\begin{aligned} \hat{H} = & \int d^3x \hat{\psi}^\dagger(x) \left(-\frac{\nabla^2}{2m} + V_{\text{ex}}(\mathbf{x}) - \mu \right) \hat{\psi}(x) \\ & + \frac{1}{2} \int d^3x d^3x' \hat{\psi}^\dagger(x) \hat{\psi}^\dagger(x') U(|\mathbf{x} - \mathbf{x}'|) \hat{\psi}(x') \hat{\psi}(x), \quad (1) \end{aligned}$$

where m and μ denote the mass of the α particle and the chemical potential, respectively. The external isotropic confinement potential $V_{\text{ex}}(\mathbf{x})$ is introduced in a phenomenological manner that will be discussed later. The interaction potential $U(r)$ is the sum of the nuclear α - α potential, $V_{\alpha-\alpha}^{\text{Nuc}}(r)$, and the Coulomb potential, $V_{\alpha-\alpha}^{\text{Coul}}(r)$. We set $\hbar = c = 1$ throughout this paper.

Assuming α condensation, namely, the broken phase, we divide $\hat{\psi}$ into a condensate c -number component ξ and an excitation component $\hat{\varphi}$ using the criterion $\langle 0 | \hat{\psi} | 0 \rangle = \xi$. The order parameter ξ is taken to be stationary, isotropic, and real, and is normalized to the condensed particle number as $\int d^3x \xi^2(\mathbf{x}) = N_0$, where we fix $N_0 = 3$ for ^{12}C below. The Hamiltonian (1) is rewritten in terms of $\hat{\varphi}$ as $\hat{H} = \hat{H}_2 + \hat{H}_{3,4}$, where

$$\begin{aligned} \hat{H}_2 = & \frac{1}{2} \int d^3x d^3x' (\hat{\varphi}^\dagger(x) - \hat{\varphi}(x)) \\ & \times \begin{pmatrix} \mathcal{L}(\mathbf{x}, \mathbf{x}') & \mathcal{M}(\mathbf{x}, \mathbf{x}') \\ -\mathcal{M}(\mathbf{x}, \mathbf{x}') & -\mathcal{L}(\mathbf{x}, \mathbf{x}') \end{pmatrix} \begin{pmatrix} \hat{\varphi}(x') \\ \hat{\varphi}^\dagger(x') \end{pmatrix}, \quad (2) \end{aligned}$$

$$\begin{aligned} \hat{H}_{3,4} = & \frac{1}{2} \int d^3x d^3x' U(|\mathbf{x} - \mathbf{x}'|) \\ & \times \{ [2\xi(\mathbf{x}') + \hat{\varphi}^\dagger(x')] \hat{\varphi}^\dagger(x) \hat{\varphi}(x) \hat{\varphi}(x') + \text{h.c.} \}, \quad (3) \end{aligned}$$

with

$$V_H(\mathbf{x}) = \int d^3x' U(|\mathbf{x} - \mathbf{x}'|) \xi^2(\mathbf{x}'), \quad (4)$$

$$\mathcal{M}(\mathbf{x}, \mathbf{x}') = U(|\mathbf{x} - \mathbf{x}'|) \xi(\mathbf{x}) \xi(\mathbf{x}'), \quad (5)$$

$$\begin{aligned} \mathcal{L}(\mathbf{x}, \mathbf{x}') = & \delta(\mathbf{x} - \mathbf{x}') (-\nabla^2/2m + V_{\text{ex}}(\mathbf{x}) \\ & - \mu + V_H(\mathbf{x})) + \mathcal{M}(\mathbf{x}, \mathbf{x}'). \quad (6) \end{aligned}$$

The requirement that the $\hat{\varphi}$ -linear term in \hat{H} must vanish leads to the Gross-Pitaevskii equation [36]

$$(-\nabla^2/2m + V_{\text{ex}}(\mathbf{x}) - \mu + V_H(\mathbf{x})) \xi(\mathbf{x}) = 0. \quad (7)$$

According to the method developed in cold atomic physics, $\hat{\varphi}$ is expanded as [37, 38]

$$\hat{\varphi}(x) = \hat{\varphi}_{\text{ex}}(x) - i\hat{Q}(t)\xi(\mathbf{x}) + \hat{P}(t)\eta(\mathbf{x}). \quad (8)$$

The field $\hat{\varphi}_{\text{ex}}(x)$ is expanded as $\hat{\varphi}_{\text{ex}}(x) = \sum_{\mathbf{n}} [\hat{a}_{\mathbf{n}}(t)u_{\mathbf{n}}(\mathbf{x}) + \hat{a}_{\mathbf{n}}^\dagger(t)v_{\mathbf{n}}^*(\mathbf{x})]$, where $u_{\mathbf{n}}$ and $v_{\mathbf{n}}$ are the elements of the Bogoliubov-de Gennes (BdG) eigenfunction [39, 40],

$$\int d^3x' \begin{pmatrix} \mathcal{L} & \mathcal{M} \\ -\mathcal{M} & -\mathcal{L} \end{pmatrix} \begin{pmatrix} u_{\mathbf{n}} \\ v_{\mathbf{n}} \end{pmatrix} = \omega_{\mathbf{n}} \begin{pmatrix} u_{\mathbf{n}} \\ v_{\mathbf{n}} \end{pmatrix}, \quad (9)$$

with a normalization condition $\int d^3x [|u_{\mathbf{n}}|^2 - |v_{\mathbf{n}}|^2] = 1$. The isotropic ξ implies $\mathbf{n} = (n, \ell, m)$, a triad of the main, azimuthal, and magnetic quantum numbers. In Eq. (8), ξ is the element of the BdG eigenfunction belonging to zero eigenvalue, and η is its adjoint function, calculated as

$$\eta(\mathbf{x}) = \frac{\partial}{\partial N_0} \xi(\mathbf{x}), \quad (10)$$

with a normalization condition $\int d^3x [\xi^* \eta + \eta^* \xi] = 1$. The CCR of $\hat{\psi}$ and $\hat{\psi}^\dagger$ yields $[\hat{a}_{\mathbf{n}}, \hat{a}_{\mathbf{n}'}^\dagger] = \delta_{\mathbf{n}\mathbf{n}'}$, $[\hat{Q}, \hat{P}] = i$, (otherwise) = 0. The pair of canonical operators \hat{Q} and \hat{P} , which are associated with the eigenfunctions with zero eigenvalue and stem from the SBS of the global phase, are counterparts of the NG and Higgs mode operators in general infinite systems. The use of the mode operators in our finite system does not diagonalize the unperturbed Hamiltonian and also causes singular behavior, whereas that of \hat{Q} and \hat{P} is free from these difficulties. We call (\hat{Q}, \hat{P}) and the subspace of states operated by them the Nambu-Goldstone-Higgs (NGH) operators and NGH subspace (or simply zero mode operators and zero mode subspace), respectively. The excitation mode created by $\hat{a}_{\mathbf{n}}^\dagger$ is referred to as the BdG mode. We note that the NGH operators exist in our finite model of superfluid type irrespective of the fact that the Higgs mode is absent in non-relativistic infinite models of this type [29].

Let us seek the vacuum $|0\rangle$, with which we identify the Hoyle state. A naive choice of the unperturbed Hamiltonian would be \hat{H}_2 , because the system is a dilute,

weakly interacting gas-like one, so the higher powers of $\hat{\varphi}$, $\hat{H}_{3,4}$ could be ignored in the leading order. Substituting Eq. (8) into Eq. (2), we obtain $\hat{H}_2 = I\hat{P}^2/2 + \sum_{\mathbf{n}} \omega_{\mathbf{n}} \hat{a}_{\mathbf{n}}^\dagger \hat{a}_{\mathbf{n}}$, with $I = \partial\mu/\partial N_0$. The Hamiltonian of the NGH operators, which has the free-particle form and therefore a continuous spectrum, causes serious defects, that is, the non-existence of a stationary normalized vacuum and the diffusing phase of ξ [37].

In the traditional formulations such as in Refs. [37] and [41], the linear expansion is replaced with the approximate non-linear expansion,

$$\hat{\psi}(x) \simeq e^{-i\hat{Q}(t)} \left\{ \xi(\mathbf{x}) + \hat{P}(t)\eta(\mathbf{x}) + \hat{\varphi}_{\text{ex}}(x) \right\} \quad (11)$$

under the assumption of small \hat{Q} . The authors of Ref. [41] specified the global properties of \hat{Q} and \hat{P} , identifying them as the azimuth angle and angular momentum operators, respectively, on the ground of the expression (11) although its validity is restricted to small \hat{Q} . As a result, the spectrum of \hat{P} and consequently that of the Hamiltonian become discrete, so one does not encounter the defects in the preceding paragraph. However, we can not accept the non-linear expansion (11) from the standpoint of quantum field theory because it violates the CCR of $\hat{\psi}$ and $\hat{\psi}^\dagger$. As will be given just below, we insist on the linear expansion (8), that is, the CCR, but introduce the non-linear unperturbed Hamiltonian instead of the bilinear one.

To avoid the defects mentioned above, a modified unperturbed Hamiltonian [34], which retains the nonlinear terms of \hat{Q} and \hat{P} in $\hat{H}_{3,4}$, has been proposed, because it is unfounded to neglect them, unlike the higher powers of the BdG modes. Concretely, we replace the term $I\hat{P}^2/2$ above with

$$\begin{aligned} \hat{H}_u^{QP} = & -(\delta\mu + 2C_{2002} + 2C_{1111})\hat{P} + \frac{I - 4C_{1102}}{2}\hat{P}^2 \\ & + 2C_{2011}\hat{Q}\hat{P}\hat{Q} + 2C_{1102}\hat{P}^3 + \frac{1}{2}C_{2020}\hat{Q}^4 - 2C_{2011}\hat{Q}^2 \\ & + C_{2002}\hat{Q}\hat{P}^2\hat{Q} + \frac{1}{2}C_{0202}\hat{P}^4, \end{aligned} \quad (12)$$

where $C_{ij\nu j'} = \int d^3x d^3x' U(r)\xi^i(\mathbf{x})\eta^j(\mathbf{x})\xi^{i'}(\mathbf{x}')\eta^{j'}(\mathbf{x}')$ with $r = |\mathbf{x} - \mathbf{x}'|$, and $\delta\mu$ is to be determined self-consistently to satisfy the criterion $\langle 0|\hat{\psi}|0\rangle = \xi$. The fact that the spectrum of \hat{H}_u^{QP} is discrete is especially significant. It is implicitly postulated in the introduction of Eq. (12) that the unperturbed state of the total system is factorized as $|\Psi\rangle|\cdot\rangle_{\text{ex}}$, where $|\Psi\rangle$ and $|\cdot\rangle_{\text{ex}}$ are a wave function in the NGH subspace and a Fock state associated with $\hat{a}_{\mathbf{n}}$, respectively. Accordingly, all the cross terms such as $\hat{a}_{\mathbf{n}}\hat{Q}\hat{P}$ are included in the interaction Hamiltonian and should be treated perturbatively. The unperturbed vacuum $|0\rangle$, which is identified with the Hoyle state, is now given by $|\Psi_0\rangle|0\rangle_{\text{ex}}$, where $|\Psi_0\rangle$ is the ground state in the NGH (zero mode) eigenequation

$$\hat{H}_u^{QP}|\Psi_\nu\rangle = E_\nu|\Psi_\nu\rangle \quad (\nu = 0, 1, \dots). \quad (13)$$

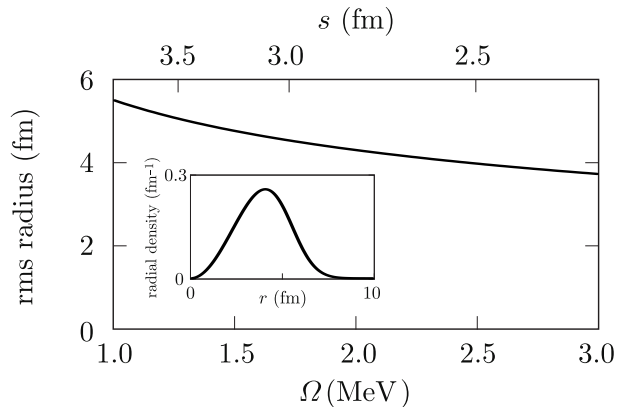


FIG. 1. Calculated \bar{r} as a function of Ω and the radial density distribution for $\Omega=2.14$ MeV (inset) of the Hoyle state. Upper horizontal axis indicates rms radius $s = \sqrt{3/2m\Omega}$ of the 0s orbit of the external harmonic oscillator potential.

The excitation in the NGH subspace is a new and original concept and our prediction, for which the adoption of the non-quadratic Hamiltonian in Eq. (12) is crucial [34]. Note that this excitation does not change the value of the angular momentum J because the NGH operators carry no quantum number in configuration space. The states $|\Psi_\nu\rangle|0\rangle_{\text{ex}}$ ($\nu = 1, 2, \dots$), which have gap energies from the Hoyle state $E_\nu - E_0$, are referred to as the *NGH states* below. The BdG excitation energy $\omega_{\mathbf{n}}$ is measured from the energy of the Hoyle state, and the state $|\Psi_0\rangle(\hat{a}_{\mathbf{n}}^\dagger|0\rangle_{\text{ex}})$ is termed the *BdG state*. Its experimental J is given by the azimuthal quantum number ℓ of \mathbf{n} . Solving the coupled system of the GP eq. (7), BdG eq. (9) with Eq. (10), and NGH (zero mode) eq. (13), we obtain theoretical predictions that can be compared with experimental data, as shown below.

III. PARAMETERS AND NUMERICAL CALCULATIONS

In the calculations, we take a phenomenological Ali-Bodmer potential for $V_{\alpha-\alpha}^{\text{Nuc1}}(r)$, which is characterized by the four parameters [35],

$$V_{\alpha-\alpha}^{\text{Nuc1}}(r) = V_r e^{-\mu_r^2 r^2} - V_a e^{-\mu_a^2 r^2}, \quad (14)$$

where V_r and V_a are the strengths of the repulsive and attractive parts, respectively, and μ_r and μ_a the corresponding inverse ranges. This potential was obtained by fitting the s -wave phase shifts of α - α scattering and has been used in three- α cluster structure studies of ^{12}C [4]. It has been a well-known fact that the Ali-Bodmer local potential does not reproduce the binding energy of the ground state and the Hoyle state. The attraction of the Ali-Bodmer potential is too weak for the three-alpha system. One way to reproduce the correct binding of these states is to introduce a strong three-body attracting

force [4, 42, 43]. Alternatively, in this paper, we introduce an external harmonic potential $V_{\text{ex}}(r) = m\Omega^2 r^2/2$ which mimics the three-body attracting force to bind the Hoyle state. Here, Ω is a fit parameter which corresponds to the strength of the three-body force. The introduction of the external potential makes the theoretical analysis simpler without losing the self-binding essence. If we took only the interaction among the alpha particles, the original translational symmetry would be spontaneously broken in the formation of the nucleus. Then we would have an additional NG mode associated with the translational symmetry in addition to the one of the phase symmetry. To avoid this complexity, we explicitly break the translational symmetry by introducing the external potential. The Coulomb potential, $V_{\alpha-\alpha}^{\text{Coul}}(r)$, is taken as $(4e^2/r)\text{erf}(\sqrt{3}r/2b)$, where the size parameter of the α particle b is 1.44 fm.

We attempt to calculate the rms radius, denoted by $\bar{r} = \sqrt{\langle r^2 \rangle}$, and density profile of the Hoyle state from $\xi(\mathbf{x})$ taking the parameter set d_0 in Ref. [35] with the proviso that the parameter V_r decreases slightly from 500 MeV to 422 MeV, which is consistent with the finding in Ref.[44] that the α - α interaction in the three- α system is more attractive than that determined in free α - α scattering. The results are shown in Fig. 1. The Hoyle state is found to be dilute for all the Ω values. The peak position of the radial density distribution, located around 4 \sim 5 fm, and \bar{r} are not very sensitive to Ω .

The coexistence of concentration by the trapping potential and repulsion by the self-interaction is crucial for a stable BEC of trapped cold atoms. As a typical counterexample, the trapped BEC of attractively interacting atoms collapses. We therefore regard Ω and V_r as the key parameters in our study, and fit them below with the fixed $V_a = 130$ MeV, $\mu_a = 0.475$ fm $^{-1}$, and $\mu_r = 0.7$ fm $^{-1}$ in the parameter set d_0 [35].

IV. ENERGY SPECTRUM

First we use only the existing experimental energy levels to determine the two fit parameters Ω and V_r . The Ω -dependence of the calculated energy levels is given in Fig. 2. Fig. 3 shows the calculated energy levels for the best fitting parameters $\Omega = 2.14$ MeV and $V_r = 422$ MeV, which is referred to as the parameter set A, in comparison with the observed α cluster states. The calculated \bar{r} of 0_2^+ is 4.21fm, which is comparable with the calculations in Refs. [2, 3, 6, 8]. The agreement between the calculated and experimental energy levels is good, and the order of the levels is correctly reproduced. Our calculation reproduces the two 0^+ NGH states ($\nu = 1, 2$), which correspond well to the 0_3^+ at 9.04 MeV and 0_4^+ at 10.56 MeV, respectively. The existence of the NGH states is critical for the assignments, because there is no BdG state with $\ell = 0$ near the energies of 0_3^+ and 0_4^+ . Then, quite naturally, the excitations 2_2^+ and 4_1^+ are identified as the BdG states with $\ell = 2, 4$. All the observed pos-

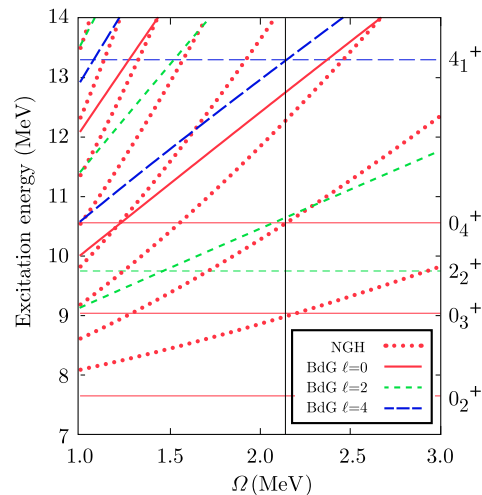


FIG. 2. (Color online) NGH (dotted lines) and BdG (solid or dashed lines) excitation energies with $\ell = 0$ (red), 2 (green), and 4 (blue) as a function of Ω when $V_r = 422$ MeV is fixed. The horizontal lines indicate the excitation energies of the observed α cluster states in ^{12}C [14–19], and the vertical line is a guide to the eye.

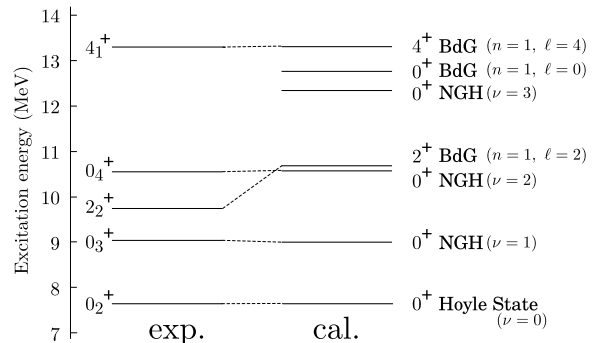


FIG. 3. The calculated energy levels for parameter set A ($\Omega = 2.14$ MeV, $V_r = 422$ MeV), compared with the observed α cluster states in ^{12}C [14–19].

itive parity states are well reproduced as BEC states of α clusters. This shows that the present field theory is useful even for a few-body system.

In Figs. 2 and 3, the calculation shows two 0^+ states around 12.5 MeV, where no corresponding excitation has been established experimentally yet. These are the NGH state with $\nu = 3$, $|\Psi_3\rangle|0\rangle_{\text{ex}}$, and the BdG state $|\Psi_0\rangle(\hat{a}_{100}^\dagger|0\rangle_{\text{ex}})$, denoted simply as $|h\rangle$ and $|\text{BdG}\rangle$, respectively. Because the energy difference between the two states is small and the interaction Hamiltonian allows mutual transitions, they mix with each other to make new two energy eigenstates. A rough estimation of diagonalizing \hat{H} in the subspace of $|h\rangle$ and $|\text{BdG}\rangle$ gives the eigenstates, $0.98|\text{BdG}\rangle - 0.18|h\rangle$ with an energy of 12.60 MeV and $0.98|h\rangle + 0.18|\text{BdG}\rangle$ with 12.20 MeV. The mixing is not remarkable here, but is generally sensitive to the energy difference. We also note that doubly ex-

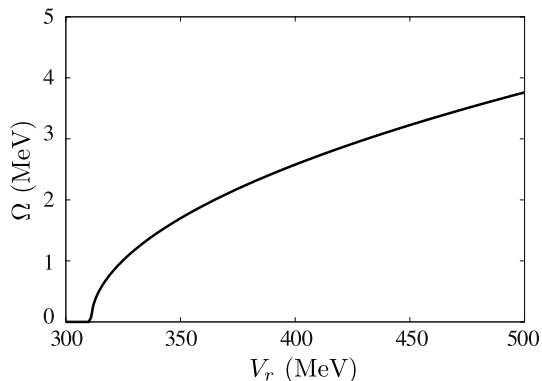


FIG. 4. V_r - Ω plot for $\bar{r} = 3.8$ fm

cited states, e.g., $|\Psi_1\rangle(\hat{a}_{02m}^\dagger|0\rangle_{ex})$ are possible.

Next, we try to determine the parameters Ω and V_r in another way. First of all, because the observed energy levels have large widths, their fitting is not very useful. We add the rms radius of the Hoyle state, depending on the wave function, as an object to be fitted. The value of $\bar{r} = 4.21$ fm, calculated for the parameter set A, is rather large, compared with the typical range $3.3 \sim 3.8$ fm obtained in other α cluster model calculations [2, 3, 9, 45, 46], and the values around 2.9 fm estimated from inelastic scattering from the Hoyle state [47]. We seek values of the parameters that give energy levels consistent with the observed energy levels, fixing \bar{r} . The plot in Fig. 4 represents a constraint when \bar{r} is fixed to be 3.8 fm. We point out the following two facts in this parameter search. Firstly, we have negative E_ν for $V_r < 370$ MeV and complex ω_{120} for $V_r < 330$ MeV, implying that BEC is unstable for smaller V_r (consequently smaller Ω). The former is caused by the negative “mass” $1/(I - 4C_{1102}) < 0$ in Eq. (12). The latter is the dynamical instability [48–54], and occurs, because the weak repulsive interaction cannot prevent BEC from collapsing. Secondly, Ω is the most significant parameter to determine the energy level spacing, and large Ω (> 3 MeV) cannot reproduce the observed energy levels. After all, no solution is found for the small \bar{r} that requires large Ω . We therefore advance our calculations, taking the maximum $\bar{r} = 3.8$ fm. Fig. 5 indicates the V_r -dependence of calculated energy levels. Choosing the best fitting parameters $\Omega = 2.58$ MeV and $V_r = 400$ MeV, called the parameter set B, we give the results of calculated energy levels in Fig. 6. The zero energy spacing are narrower due to the smaller V_r and the BdG energy spacing is wider due to the larger Ω than those in Fig. 3. As a result, the NGH state with $\nu = 4$ is located near 4_1^+ , while the energy level of the NGH state with $\nu = 3$ falls down to the midpoint between 0_4^+ and 4_1^+ , and the calculated BdG excitation levels tend to be above the observed levels.

Our interpretation of the α cluster states as phase locking due to BEC is quite different from the traditional α cluster model, *ab initio* calculations, and other approaches that try to explain them as collective modes

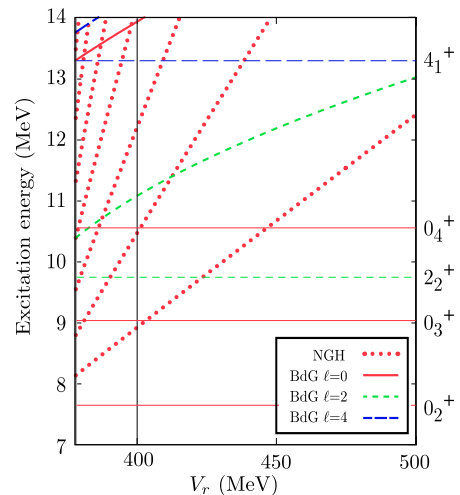


FIG. 5. (Color online) NGH (dotted lines) and BdG (solid or dashed lines) excitation energies with $\ell = 0$ (red), 2 (green), and 4 (blue) as a function of V_r for fixed $\bar{r} = 3.8$ fm.

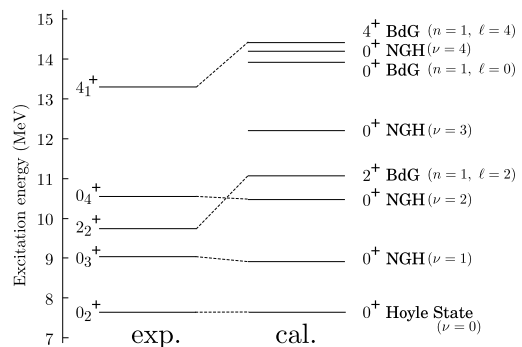


FIG. 6. The calculated energy levels for parameter set B ($\Omega = 2.58$ MeV, $V_r = 400$ MeV).

in *configuration space*, e.g., the rotational band or vibrational states caused by breakdown of rotational or translational symmetries.

In the traditional models, there has been a long-standing question about which excited states are the rotational band members built on the Hoyle state [21]. In other words, which of the 0_2^+ and 0_3^+ states is the bandhead of the observed 2_2^+ and 4_1^+ states? The first and traditional α cluster model picture regards the Hoyle state as the bandhead state [20, 55, 56]. In the α condensate model [6], the 2_2^+ state is interpreted as a state in which an α cluster is lifted from the Hoyle state to the D state in *configuration space*, and both states have essentially the same weakly coupled $[^8\text{Be}(0^+) \times \alpha]_J$ cluster configuration revealed in Refs.[2, 8]. In these cluster model pictures, because the Hoyle and 2_2^+ states have a gas-like spherical structure, it is difficult to consider logically that a rotational band is built. In *ab initio* lattice [13] and no-core shell model [12] calculations, the Hoyle, 2_2^+ , and 4_1^+ states are understood to be rotational band states. The second interpretation is that the 0_3^+ state is a bandhead

state on which the rotational 2_2^+ and 4_1^+ states are built [55]. Ref.[8] suggests that the 0_3^+ state is a higher nodal state with the $[^8\text{Be}(0^+) \times \alpha(L=0)]_{J=0}$ structure. A calculated large $B(E2)$ value of the $2_2^+ \rightarrow 0_3^+$ transition [9] is reported, although no experimental data are available. In the next section, we will calculate the transition probability and also obtain a large value in our approach.

The reason that these two different interpretations have been presented is entirely due to the appearance of the Hoyle and 0_3^+ states so closely above the α threshold. If rotational invariance of the 0_2^+ and 0_3^+ states in configuration space is broken, a rotational band should appear individually on both the 0_2^+ and 0_3^+ states, in contradiction with the experimental data. It seems difficult to determine which interpretation is correct as long as these are considered as collective modes with α cluster structure in *configuration space*. In our picture above, the question does not arise in principle. Our calculations show that the 2_2^+ and 4_1^+ states are the BdG states and need not be rotational member states on either the Hoyle state or the 0_3^+ state. In fact, the $J(J+1)$ plot of the excitation energy of the observed states of the band based on the above two pictures deviates from a straight line.

Why and how does nature allow in principle the emergence of the 0_4^+ state, which is interpreted as a linear chain-like α cluster state in Refs.[8–10, 57], so close to the 0_3^+ and 0_2^+ states? In our picture, the close 0_3^+ and 0_4^+ states emerge naturally and fundamentally as the NGH states, which is a logical consequence of BEC of the Hoyle state, and the three are closely interrelated.

V. γ DECAY

We can calculate the γ decay transitions, using the wave functions that have already been obtained. Below the transitions $2_2^+ \rightarrow 0_2^+$ and $2_2^+ \rightarrow 0_3^+$ are considered.

The interaction of α particle, treated as a point-like particle with a charge $2e$, with the photon field $\hat{\mathbf{A}}$, is introduced from the gauge principle $\nabla \rightarrow \nabla - 2ie\hat{\mathbf{A}}$ in the Hamiltonian (1), and the interaction Hamiltonian is given by

$$\hat{H}_A \simeq - \int d^3x \hat{\mathbf{j}}(x) \cdot \hat{\mathbf{A}}(x), \quad (15)$$

$$\hat{\mathbf{j}}(x) = \hat{\psi}^\dagger(x) \frac{2e}{im} \nabla \hat{\psi}(x). \quad (16)$$

We make a multipole expansion of $\hat{\mathbf{A}}$. The transitions $2_2^+ \rightarrow 0_2^+$ and $2_2^+ \rightarrow 0_3^+$ are electric quadrupole transitions, and the decay rate for a general electric transition with a photon angular momentum J is

$$\Gamma_{fi}(\mathbf{E} : k, J, M) = \frac{8\pi(J+1)}{J((2J+1)!!)^2} k^{2J+1} \times \left| \langle f | \hat{\mathcal{M}}(\mathbf{E} : kJM) | i \rangle \right|^2, \quad (17)$$

where $|i\rangle$, $|f\rangle$ represent the initial and final states of the nucleus with respective energies, E_i and E_f , and $k =$

$E_i - E_f$ is the photon energy. The multipole moment $\hat{\mathcal{M}}$ [58] is

$$\hat{\mathcal{M}}(\mathbf{E} : kJM) = \frac{(2J+1)!!}{k^{J+1}} \sqrt{\frac{J}{J+1}} \times \int d^3x \hat{\mathbf{j}}(\mathbf{x}) \cdot \nabla \times \{j_J(kr) \mathbf{Y}_{JJM}(\theta, \varphi)\}, \quad (18)$$

where j_ℓ and \mathbf{Y}_{JJM} are the spherical Bessel function and vector spherical harmonics, respectively. When the initial nuclear state is unpolarized and a sum over the final polarization states is taken, the decay rate is

$$\bar{\Gamma}_{fi}(\mathbf{E} : k, J) = \frac{8\pi(J+1)}{J((2J+1)!!)^2} k^{2J+1} B(\mathbf{E}J : J_i \rightarrow J_f) B(\mathbf{E}J : J_i \rightarrow J_f) \times \left| \langle f(J_f) | \hat{\mathcal{M}}(\mathbf{E} : kJ) | i(J_i) \rangle \right|^2, \quad (19)$$

where J_i and J_f are the initial and final nuclear spins, respectively, and B is the reduced transition probability [58].

We calculate $\bar{\Gamma}_{fi}$ and B for the transitions $2_2^+ \rightarrow 0_2^+$ and $2_2^+ \rightarrow 0_3^+$. The states 0_2^+ , 0_3^+ , and 2_2^+ are identified as the vacuum $|\Psi_0\rangle|0\rangle_{\text{ex}}$, the NGH state $|\Psi_1\rangle|0\rangle_{\text{ex}}$, and the BdG state $|\Psi_0\rangle(\hat{a}_{02m}^\dagger|0\rangle_{\text{ex}})$, respectively. Substituting $\hat{\psi} = \xi + \hat{\varphi}$ in Eq. (8) into $\hat{\mathbf{j}}$ in (16), we have the following matrix elements,

$$\begin{aligned} & \langle f(J_f = 0, M_f = 0) | \hat{\mathcal{M}}(\mathbf{E} : k20) | i(J_i = 2, M_i = 0) \rangle \\ &= \frac{30e}{imk^3} \sqrt{\frac{2}{3}} \int d^3x \langle \begin{Bmatrix} \Psi_0 \\ \Psi_1 \end{Bmatrix} | \left\{ (1 + i\hat{Q}) \xi(\mathbf{x}) + \hat{P}\eta(\mathbf{x}) \right\} \\ & \quad \times \nabla u_{120}(\mathbf{x}) + v_{120}(\mathbf{x}) \nabla \left\{ (1 - i\hat{Q}) \xi(\mathbf{x}) + \hat{P}\eta(\mathbf{x}) \right\} \\ & \quad | \Psi_0 \rangle \cdot \nabla \times \{j_2(kr) \mathbf{Y}_{220}(\theta, \varphi)\}, \end{aligned} \quad (20)$$

which are further simplified for $2_2^+ \rightarrow 0_2^+$ as

$$\begin{aligned} & \langle f(0, 0) | \hat{\mathcal{M}}(\mathbf{E} : k20) | N(2, 0) \rangle \\ &= \frac{60e}{mk^3} \int dr r \left[\xi(r) \left\{ \frac{d}{dr} \mathcal{U}_{12}(r) j_2(kr) \right. \right. \\ & \quad \left. \left. + \mathcal{U}_{12}(r) \left(\frac{j_2(kr)}{r} + k j_2'(kr) \right) \right\} \right. \\ & \quad \left. + \frac{d}{dr} \xi(r) \mathcal{V}_{12}(r) j_2(kr) \right], \end{aligned} \quad (21)$$

and for $2_2^+ \rightarrow 0_3^+$ as

$$\begin{aligned} & \langle f(0, 0) | \hat{\mathcal{M}}(\mathbf{E} : k20) | i(2, 0) \rangle \\ &= \frac{60e}{mk^3} \int dr r \left[\left\{ i \langle \Psi_1 | \hat{Q} | \Psi_0 \rangle \xi(r) + \langle \Psi_1 | \hat{P} | \Psi_0 \rangle \eta(r) \right\} \right. \\ & \quad \times \left\{ \frac{d}{dr} \mathcal{U}_{12}(r) j_2(kr) + \mathcal{U}_{12}(r) \left(\frac{j_2(kr)}{r} + k j_2'(kr) \right) \right\} \\ & \quad \left. + \left\{ i \langle \Psi_1 | \hat{Q} | \Psi_0 \rangle \frac{d}{dr} \xi(r) + \langle \Psi_1 | \hat{P} | \Psi_0 \rangle \frac{d}{dr} \eta(r) \right\} \right. \\ & \quad \left. \times \mathcal{V}_{12}(r) j_2(kr) \right]. \end{aligned} \quad (22)$$

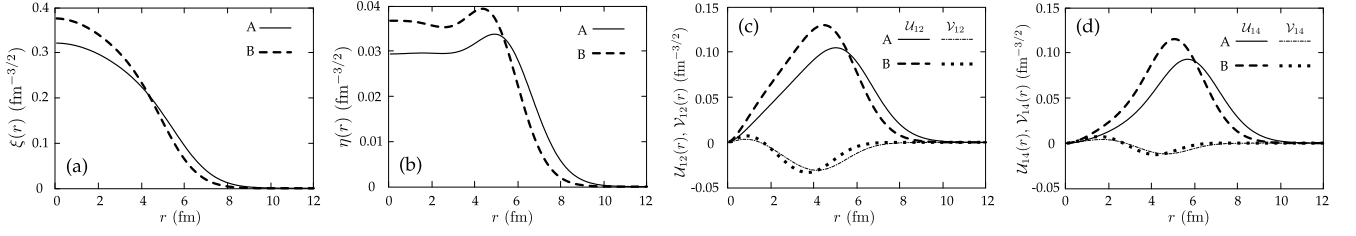


FIG. 7. Numerical solutions of (a) $\xi(r)$, (b) $\eta(r)$, (c) $\mathcal{U}_{12}(r)$, $\mathcal{V}_{12}(r)$, and (d) $\mathcal{U}_{14}(r)$, $\mathcal{V}_{14}(r)$ for the parameter sets A and B.

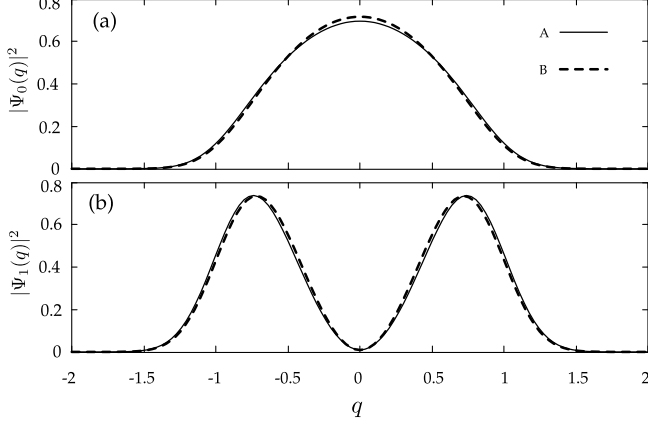


FIG. 8. Calculated $|\Psi_\nu(q)|^2$ for the parameter sets A and B.

Here note that $\langle \Psi_0 | \hat{Q} | \Psi_0 \rangle = \langle \Psi_0 | \hat{P} | \Psi_0 \rangle = 0$ but $\langle \Psi_1 | \hat{Q} | \Psi_0 \rangle, \langle \Psi_1 | \hat{P} | \Psi_0 \rangle \neq 0$, and that the radial functions are defined as

$$\begin{cases} \xi(\mathbf{x}) \\ \eta(\mathbf{x}) \end{cases} = \begin{cases} \xi(r) \\ \eta(r) \end{cases} Y_{00}(\theta, \varphi), \\ \begin{cases} u_{nJM}(\mathbf{x}) \\ v_{nJM}(\mathbf{x}) \end{cases} = \begin{cases} \mathcal{U}_{nJ}(r) \\ \mathcal{V}_{nJ}(r) \end{cases} Y_{JM}(\theta, \varphi). \quad (23)$$

Using the numerical solutions, $\xi(r)$, $\eta(r)$, $\mathcal{U}_{12}(r)$, $\mathcal{V}_{12}(r)$ and $\Psi_\nu(q) = \langle q | \Psi_\nu \rangle$ ($\nu = 0, 1$) for each of the parameter sets A and B, we obtain the reduced transition probabilities that are summarized in Table I. The solutions for each parameter set are shown in Figs. 7 and 8.

TABLE I. Calculated reduced transition probabilities $B(E2 : 2 \rightarrow 0)$ in unit of $e^2 \text{fm}^4$: Ref. [9], Ref. [59], and our results for the parameter sets A and B.

Transition	Ref. [9]	Ref. [59]	Ours (A)	Ours (B)
$2_2^+ \rightarrow 0_2^+$	100	295-340	290	204
$2_2^+ \rightarrow 0_3^+$	310	88-220	342	187

It is remarked that the process $2_2^+ \rightarrow 0_3^+$ is the transition between the NGH states, whereas the process $2_2^+ \rightarrow 0_2^+$ is the transition between the BdG states. The physical picture of condensation in our approach implies that the widths of the wave functions, especially $\eta(r)$ and

$\mathcal{U}_{12}(r)$, are large. But the final results of $B(E2 : 2 \rightarrow 0)$ are comparable with those in the other calculations, as in Table I.

VI. SUMMARY

To summarize, we have studied the α cluster structure above the α condensate Hoyle state in ^{12}C by formulating an effective field theory of α cluster condensation that properly treats spontaneous symmetry breaking of the global phase. The observed well-developed α cluster states, i.e., the 0_3^+ (9.04 MeV), 2_2^+ (9.75 MeV), 0_4^+ (10.56 MeV), and 4_1^+ (13.3 MeV) states, are well reproduced. Then, the emergence of the NGH states just above the Hoyle state is essential. The fact that excitation energies of the BdG and NGH states are the almost same order of magnitude in our calculation is also important for the energy spectrum of ^{12}C . We adopted the two parameter sets, and both are consistent with the observed spectrum that has large widths of the energy levels.

We also calculated the γ transitions, using the obtained wave functions. Our results of the reduced transition probabilities are compared with those of the other model calculations, and are consistent with the latter.

Although the α cluster condensation involves the small number of α particles, it is stable in our study. This is not true in general, and actually, when the repulsive interaction is weak, we have negative energy of the NGH state and complex energy of the BdG state that indicate an instability of the condensation.

It would be also intriguing to study the NGH states in other nuclei such as ^{16}O , ^{20}Ne , and ^{40}Ca .

ACKNOWLEDGMENTS

We thank Yasuhiro Nagai and Ryo Yoshioka for their numerical calculations, and the Yukawa Institute for Theoretical Physics at Kyoto University, where our collaboration started at the YITP workshop YITP-W-13-13 on ‘‘Thermal Quantum Field Theories and Their Applications.’’ This work is partially supported by JSPS KAKENHI Grant Nos. 25400410, 16K05488, and by a Waseda University Grant for Special Research Projects (Project No. 2014S-080).

-
- [1] E. A. Cornell and C. E. Wieman, *Rev. Mod. Phys.* **74**, 875 (2002).
- [2] E. Uegaki, S. Okabe, Y. Abe, and H. Tanaka, *Prog. Theor. Phys.* **57**, 1262 (1977); E. Uegaki, Y. Abe, S. Okabe, and H. Tanaka, *Prog. Theor. Phys.* **62**, 1621 (1979).
- [3] A. Tohsaki, H. Horiuchi, P. Schuck, and G. Ropke, *Phys. Rev. Lett.* **87**, 192501 (2001).
- [4] T. Yamada and P. Schuck, *Phys. Rev. C* **69**, 024309 (2004).
- [5] S. Ohkubo and Y. Hirabayashi, *Phys. Rev. C* **70**, 041602 (R) (2004); Sh. Hamada, Y. Hirabayashi, N. Burtbayev, and S. Ohkubo, *Phys. Rev. C* **87**, 024311 (2013).
- [6] T. Yamada and P. Schuck, *Eur. Phys. J. A* **26**, 185 (2005).
- [7] C. Kurokawa and K. Katō, *Phys. Rev. C* **71**, 021301 (2005); *Nucl. Phys. A* **738**, 455c (2004).
- [8] C. Kurokawa and K. Katō, *Nucl. Phys. A* **792**, 87 (2007).
- [9] Y. Kanada-En'yo, *Prog. Theor. Phys.* **117**, 655 (2007).
- [10] M. Chernykh, H. Feldmeier, T. Neff, P. vonNeumann-Cosel, and A. Richter, *Phys. Rev. Lett.* **98**, 032501 (2007).
- [11] R. Roth, J. Langhammer, A. Calci, S. Binder, and P. Navratil, *Phys. Rev. Lett.* **107**, 072501 (2011).
- [12] A. C. Dreyfuss, K. D. Launey, T. Dytrych, J. P. Draayer, and C. Bahri, *Phys. Lett. B* **727**, 515 (2013).
- [13] E. Epelbaum, H. Krebs, T. A. Lahde, D. Lee, and Ulf-G. Meissner, *Phys. Rev. Lett.* **109**, 252501 (2012).
- [14] M. Freer *et al.*, *Phys. Rev. C* **80**, 041303(R) (2009).
- [15] M. Itoh *et al.*, *Nucl. Phys. A* **738**, 268 (2004); M. Itoh *et al.*, *Phys. Rev. C* **84**, 054308 (2011).
- [16] W. R. Zimmerman, N. E. Destefano, M. Freer, M. Gai, and F. D. Smit, *Phys. Rev. C* **84**, 027304 (2011).
- [17] W. R. Zimmerman *et al.*, *Phys. Rev. Lett.* **110**, 152502 (2013).
- [18] M. Itoh *et al.*, *J. Phys.: Conf. Ser.* **436**, 012006 (2013).
- [19] M. Freer *et al.*, *Phys. Rev. C* **83**, 034314 (2011).
- [20] A. A. Ogloblin *et al.*, *EPJ Web Conf.* **66**, 02074 (2014).
- [21] M. Freer and H. O. U. Fymbo, *Prog. Part. Nucl. Phys.* **78**, 1 (2014).
- [22] P. Ring and P. Schuck, *The Nuclear Many-body Problem*, (Springer-Verlag, Berlin, 1980).
- [23] J. P. Blaizot and G. Ripka, *Quantum Theory of Finite Systems*, (MIT press, Cambridge, 1985).
- [24] H. Watanabe and H. Murayama, *Phys. Rev. Lett.* **108**, 251602 (2012); Y. Hidaka, *Phys. Rev. Lett.* **110**, 091601 (2013).
- [25] Y. Nambu and G. Jona-Lasinio, *Phys. Rev.* **122**, 345 (1961).
- [26] J. Goldstone, *Nuovo Cimento* **19**, 154 (1961).
- [27] K. Kadowaki, I. Takeya, and K. Kindo, *Europhys. Lett.* **42**, 203 (1998).
- [28] P. B. Littlewood and C. M. Varma, *Phys. Rev. Lett.* **47**, 811 (1981); P. B. Littlewood and C. M. Varma, *Phys. Rev. B* **26**, 4883 (1982).
- [29] C. M. Varma, *J. Low Temp. Phys.* **126**, 901 (2001).
- [30] R. A. Broglia, O. Hansen, and C. Riedel, *Adv. Nucl. Phys.* **6**, 259 (1973); R. A. Broglia, J. Terasaki, and N. Giovanardi, *Phys. Rep.* **335**, 1 (2000); D. M. Brink and R. A. Broglia, *Nuclear Superfluidity: Pairing in Finite Systems* (Cambridge University Press, Cambridge, 2005).
- [31] ATLAS Collaboration, *Phys. Lett. B* **716**, 1 (2012); CMS Collaboration, *Phys. Lett. B* **716**, 30 (2012).
- [32] R. Matsunaga, Y. I. Hamada, K. Makise, Y. Uzawa, H. Terai, Z. Wang, and R. Shimano, *Phys. Rev. Lett.* **111**, 057002 (2013).
- [33] S. Ohkubo, arXiv: nucl-th 1301.7485 (2013).
- [34] Y. Nakamura, J. Takahashi, and Y. Yamanaka, *Phys. Rev. A* **89**, 013613 (2014).
- [35] S. Ali and A. R. Bodmer, *Nucl. Phys. A* **80**, 99 (1966).
- [36] E. P. Gross, *Nuovo Cimento* **20**, 454 (1961); *J. Math. Phys.* **4**, 195 (1963); L. P. Pitaevskii, *Zh. Eksp. Teor. Fiz.* **40**, 646 (1961).
- [37] M. Lewenstein and L. You, *Phys. Rev. Lett.* **77**, 3489 (1996).
- [38] H. Matsumoto and S. Sakamoto, *Prog. Theor. Phys.* **107**, 679 (2002).
- [39] N. N. Bogoliubov, *J. Phys. (Moscow)* **11**, 32 (1947).
- [40] P. G. de Gennes, *Superconductivity of Metals and Alloys* (Benjamin, New York, 1966).
- [41] E.R. Marshalek and J. Weneser, *Ann. Phys.* **53**, 569 (1969).
- [42] H. Ogasawara and J. Hiura, *Prog. Theor. Phys.* **59**, 655 (1978).
- [43] R. Lazauskas and M. Dufour, *Phys. Rev. C* **84**, 064318 (2011).
- [44] A. Tohsaki-Suzuki, M. Kamimura, and K. Ikeda, *Prog. Theor. Phys. Suppl.* **68**, 359 (1978).
- [45] M. Kamimura, *Nucl. Phys. A* **351**, 456 (1981).
- [46] H. Matsumura and Y. Suzuki, *Nucl. Phys. A* **739**, 238 (2004).
- [47] A. N. Danilov, T. L. Belyaeva, A. S. Demyanova, S. A. Goncharov, and A. A. Ogloblin, *Phys. Rev. C* **80**, 054603 (2009).
- [48] H. Pu, C. K. Law, J. H. Eberly, and N. P. Bigelow, *Phys. Rev. A* **59**, 1533 (1999).
- [49] L. J. Garay, J. R. Anglin, J. I. Cirac, and P. Zoller, *Phys. Rev. Lett.* **85**, 4643, (2000); *Phys. Rev. A* **63**, 023611 (2001).
- [50] D. V. Skryabin, *Phys. Rev. A* **63**, 013602 (2000).
- [51] B. Wu and Q. Niu, *New J. Phys.* **5**, 104 (2003).
- [52] M. Möttönen, T. Mizushima, T. Isoshima, M. M. Salomaa, and K. Machida, *Phys. Rev. A* **68**, 023611 (2003).
- [53] Y. Kawaguchi and T. Ohmi, *Phys. Rev. A* **70**, 043610 (2004).
- [54] M. Mine, M. Okumura, T. Sunaga and Y. Yamanaka, *Ann. Phys.* **322**, 2327 (2007).
- [55] M. Freer, *J. Phys.: Conf. Ser.* **436**, 012002 (2013).
- [56] H. Morinaga, *Phys. Rev.* **101**, 254 (1956).
- [57] T. Suhara, Y. Funaki, B. Zhou, H. Horiuchi, and A. Tohsaki, *Phys. Rev. Lett.* **112**, 062501 (2014).
- [58] A. Bohr and B. R. Mottelson, *Nuclear Structure Vol. I*, (Benjamin, New York, 1969).
- [59] Y. Funaki, *Phys. Rev. C* **92**, 021302(R) (2015).